5320 J. Med. Chem. 2010, 53, 5320–5332
DOI: 10.1021/jm100541c

Journal of Medicinal Chemistry Article

Discovery of the Dual Orexin Receptor Antagonist [(7*R*)-4-(5-Chloro-1,3-benzoxazol-2-yl)-7-methyl-1,4-diazepan-1-yl][5-methyl-2-(2*H*-1,2,3-triazol-2-yl)phenyl]methanone (MK-4305) for the Treatment of Insomnia

Christopher D. Cox,*[,†] Michael J. Breslin,[†] David B. Whitman,[†] John D. Schreier,[†] Georgia B. McGaughey,[‡] Michael J. Bogusky,[†] Anthony J. Roecker,[†] Swati P. Mercer,[†] Rodney A. Bednar,[§] Wei Lemaire,[§] Joseph G. Bruno,[§] Duane R. Reiss,[∥] C. Meacham Harrell,[∥] Kathy L. Murphy,[∥] Susan L. Garson,[∥] Scott M. Doran,[∥] Thomayant Prueksaritanont,[⊥] Wayne B. Anderson,[⊥] Cuyue Tang,[⊥] Shane Roller,[⊥] Tamara D. Cabalu,[⊥] Donghui Cui,[⊥] George D. Hartman,[†] Steven D. Young,[†] Ken S. Koblan,[∥] Christopher J. Winrow,[∥] John J. Renger,[∥] and Paul J. Coleman[†]

[†]*Departments of Medicinal Chemistry,* [‡]*Chemistry Modeling and Informatics,* [§]*In Vitro Sciences,* [∥]*Depression and Circadian Disorders, and* [⊥]*Drug Metabolism, Merck Research Laboratories, P.O. Box 4, Sumneytown Pike, West Point, Pennsylvania 19486*

Received May 5, 2010

Despite increased understanding of the biological basis for sleep control in the brain, few novel mechanisms for the treatment of insomnia have been identified in recent years. One notable exception is inhibition of the excitatory neuropeptides orexins A and B by design of orexin receptor antagonists. Herein, we describe how efforts to understand the origin of poor oral pharmacokinetics in a leading HTS-derived diazepane orexin receptor antagonist led to the identification of compound **10** with a 7-methyl substitution on the diazepane core. Though **10** displayed good potency, improved pharmacokinetics, and excellent in vivo efficacy, it formed reactive metabolites in microsomal incubations. A mechanistic hypothesis coupled with an in vitro assay to assess bioactivation led to replacement of the fluoroquinazoline ring of **10** with a chlorobenzoxazole to provide **3** (MK-4305), a potent dual orexin receptor antagonist that is currently being tested in phase III clinical trials for the treatment of primary insomnia.

Introduction

Insomnia is characterized by difficulty initiating and/or maintaining sleep, waking early, or finding sleep nonrestorative. In a recent poll of American adults, over 50% reported having at least one symptom of insomnia during the previous year, and a third reported symptoms almost every night.[1] Insomnia is considered primary if no known underlying mental or physical condition leads to its development, and has been directly linked to significant daytime consequences such as irritability, inability to concentrate, reduced energy levels, poor job performance, work absenteeism, and a greater risk of traffic and work-related accidents as well as a higher incidence of health problems.[1,2] Insomnia is also commonly experienced as a secondary symptom of comorbid disorders. The direct and indirect costs to the US economy related to insomnia have been estimated to be well in excess of $100 billion per year.[3] It is believed that a significant number of cases go undiagnosed and/or untreated due to an opinion by many sufferers that sleep problems are inconsequential and a pervasive belief by physicians that currently available treatments have questionable safety and efficacy.[1] Notwithstanding, one-quarter of American adults take sleep medications during the course of a year, and the U.S. market for sleep drugs is estimated to reach $5 billion per year by 2010.[3a]

Despite the physical, psychological, and economic toll of insomnia, treatments that improve total sleep time and subjective sleep quality without risk of next-day impairment, dependence, rebound insomnia, or safety concerns remain elusive.[4] The most widely prescribed agents for treatment of insomnia are central nervous system depressants that enhance signaling of the inhibitory neurotransmitter γ-aminobutyric acid (GABA[a]). Developed beginning in the early 1960s, benzodiazepines decrease sleep onset time by binding to $GABA_A$ receptors on postsynaptic neurons in the central nervous system but are associated with issues such as daytime sleepiness, dizziness, impaired memory, and risk of dependence.[1] The subtype selective benzodiazepine and nonbenzodiazepine $GABA_A$ modulators developed more recently, such as zolpidem, zaleplon, and eszopiclone, address some of the issues associated with earlier agents but questions remain about the overall safety and efficacy of these agents.[3] The FDA recently mandated black-box warnings related to the safety profile of all sedative hypnotics, underscoring the agency's concern with the currently available treatments.[5] In 2005, the FDA approved the melatonin receptor antagonist ramelteon for the treatment of insomnia, representing the first novel mechanism to be approved in 35 years and the only hypnotic not classified as a

*To whom correspondence should be addressed. Phone: + 1-215-652-2411. Fax: + 1-215-652-7310. E-mail: chris_cox@merck.com.

[a] Abbreviations: BDC, bile-duct cannulated; Boc, *tert*-butoxycarbonyl; BSA, bovine serum albumin; CSF, cerebrospinal fluid; DORA, dual orexin receptor antagonist; ECoG, electrocorticogram; EMG, electromyogram; FLIPR, fluorometric imaging plate reader; GABA, γ-aminobutyric acid; GSH, glutathione; ICV, intracerebroventricular; LPS, latency to persistent sleep; NSB, nonspecific binding; OTC, over-the-counter; OX_1R, orexin receptor 1; OX_2R, orexin receptor 2; PEG, polyethylene glycol; REM, rapid-eye movement; SORA, selective orexin receptor antagonist; SWS, slow-wave sleep; TB, total binding; TPGS, D-α-tocopheryl polyethylene glycol-100-succinate; WASO, wake after sleep onset.

 Published on Web 06/21/2010

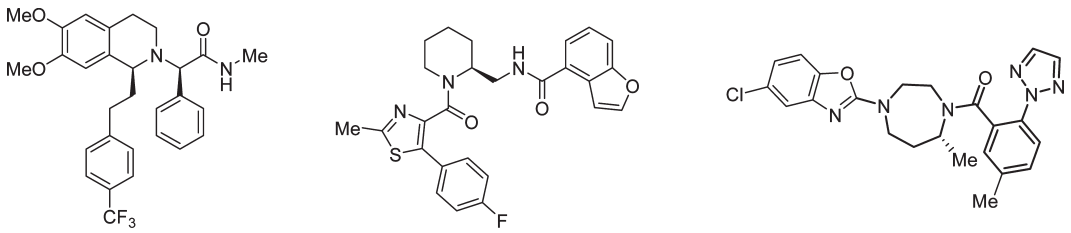

1 (Almorexant) **2** (SB-649868) **3** (MK-4305)

Figure 1. DORAs studied to date in clinical trials.

controlled substance.[6] However, questions remain about the effectiveness of ramelteon relative to $GABA_A$ modulators.[7] Clearly, novel mechanisms for the treatment of insomnia that simultaneously address the need for improved safety and efficacy are of great interest, and an increased understanding of the neuronal circuitry involved in the sleep/wake cycle has spurred a rational search for such targets.

One of the most promising discoveries in this regard is the orexin (or hypocretin) system that is highly conserved across species and intricately linked to the regulation of sleep and wake states.[8] Orexins A and B are neuropeptides derived from the same prepro-orexin peptide that is produced in neurons located in the lateral hypothalamus. These neurons project widely to regions of the brain involved in regulation of arousal. Discovered in 1998 by independent research groups, the orexin peptides were found to bind to the previously identified orphan G protein-coupled receptors, orexin receptor 1 (OX_1R) and orexin receptor 2 (OX_2R).[9] Whereas OX_1R binds orexin A with greater affinity than orexin B, OX_2R binds to both peptides with equal affinity.

A number of genetic and pharmacological studies have confirmed the central role that orexin signaling plays in regulation of the sleep/wake cycle. Mice engineered to be deficient in orexin peptides demonstrate a robust phenotype consistent with human narcolepsy, a sleep disorder characterized by excessive daytime sleepiness, sleep fragmentation, and abnormal transitions to REM sleep.[10] Selective knockout of OX_1R in mice revealed a mild phenotype characterized by sleep fragmentation, whereas knockout of OX_2R produced a narcoleptic phenotype but one that is less severe than the peptide knockout. Simultaneous knockout of both OX_1R and OX_2R produced an acute narcoleptic phenotype similar to the peptide-deficient animals.[11] Additionally, a colony of dogs that naturally suffer from narcolepsy possess a mutation in the gene coding for the OX_2R,[12] whereas the disorder in humans has been linked to a reduction of orexin-producing neurons, resulting in low or undetectable levels of orexin A in the cerebrospinal fluid (CSF) of narcoleptics.[13] Consistent with these observations, direct intracerebroventricular (ICV) infusion of the orexin peptides into rat CSF leads to an increase in arousal and a decrease in REM and non-REM sleep.[14]

Because hypofunction of the orexin system leads to decreased wakefulness, orexin receptor antagonists have emerged as a potential target for the treatment of insomnia as well as conditions resulting from disruption of the natural circadian cycle such as shift work or jet lag.[15] However, on the basis of genetic studies, the potential for orexin receptor blockade to cause cataplexy, a condition closely linked to a subset of narcolepsy sufferers and characterized by sudden loss of muscle tone, was identified as a potential concern. A number of laboratories therefore embarked on a search for selective (OX_1R or OX_2R) as well as dual (OX_1R/OX_2R) orexin receptor antagonists to better characterize their therapeutic potential. These efforts have resulted in identification of potent dual orexin receptor antagonists (DORAs) as well as selective orexin receptor antagonists (SORAs) that have enabled pharmacological studies of their in vivo activity.[15c,d,16] Most work to date has focused on DORAs, likely due to the fact that genetic studies suggested a more robust effect on the sleep/wake cycle when both receptors are affected;[11] however, a recent publication revealed that an OX_2R-selective SORA promotes sleep in rats.[17]

The most fully characterized DORA studied to date is (2*R*)-2-[(1*S*)-6,7-dimethoxy-1-{2-[4-(trifluoromethyl)phenyl]ethyl}-3,4-dihydroisoquinolin-2(1*H*)-yl]-*N*-methyl-2-phenylethanamide (**1**, Almorexant), a compound currently in phase III clinical trials for the treatment of primary insomnia (Figure 1).[18] Developed by Actelion Pharmaceuticals, it has been shown to significantly decrease wakefulness in rats, dogs, and humans, with no evidence of cataplexy.[19] In a phase II trial, Almorexant provided clinical proof of concept for the orexin antagonist mechanism in the treatment of insomnia, improving sleep efficiency in primary insomniacs, and showing no significant next-day effects on motor function or reaction time.[20] The second entry into the clinic was the DORA *N*-{[(2*S*)-1-{[5-(4-fluorophenyl)-2-methyl-1,3-thiazol-4-yl]carbonyl}piperidin-2-yl]methyl}-1-benzofuran-4-carboxamide (**2**, SB-649868) from GlaxoSmithKline. It showed positive results in terms of efficacy without residual next day effects; however, preclinical toxicology findings have delayed advancement of this compound.[21] Importantly, both compounds have been shown to induce a natural sleep architecture characterized by increases in the time spent in REM and non-REM sleep, differentiating them from $GABA_A$ modulators such as zolpidem that reduce time spent in these sleep stages believed to be important for consolidation of memory and the restorative functions of sleep.[15c] In December 2008, Merck presented preliminary phase I results indicating that DORA [(7*R*)-4-(5-chloro-1,3-benzoxazol-2-yl)-7-methyl-1,4-diazepan-1-yl]-[5-methyl-2-(2*H*-1,2,3-triazol-2-yl)phenyl]methanone (**3**, MK-4305) decreased latency to persistent sleep (LPS) and wake after sleep onset (WASO), with no disruption of sleep architecture, in healthy volunteers.[22]

The favorable clinical results obtained with three structurally diverse DORAs underscores the promise that orexin receptor antagonism holds for the treatment of sleep disorders. In this article, we describe the discovery and preclinical profile of **3**, a potent brain-penetrant DORA that recently entered phase III clinical trials for the treatment of primary insomnia.[23]

Results and Discussion

A recent publication from our group described the discovery of **4**, a novel diazepane-based DORA identified by hit-to-lead efforts following high throughput screening of the

Merck sample collection (Figure 2).[24] Compound **4** demonstrates low nanomolar affinity for the human OX_1R and OX_2R as measured by a radioligand-displacement binding assay (expressed as K_i), as well as excellent potency in a fluorometric imaging plate reader (FLIPR) assay that provides a functional readout of orexin receptor antagonism in CHO cells engineered to overexpress the human receptors (expressed as IC_{50}). It was found to promote sleep in rats when dosed orally at 100 mg/kg by increasing the amount of time spent in both REM and delta sleep.[25] This observation is consistent with the profile of clinically studied DORAs **1** and **2**[15c] and opposite to the effect seen following ICV administration of the native peptide.[14]

Though **4** has excellent brain penetration, good physical properties, a clean ancillary profile, and produces desired effects on sleep architecture, it suffers from high clearance and low bioavailability in the rat (Table 1). In the dog, **4** displays moderate plasma clearance (11.6 mL/min/kg) but low bioavailability (16%). In light of the observed clearance (calculated blood clearance accounts for ~50% of hepatic blood flow), maximal bioavailability is anticipated to be ~50% in dog assuming complete absorption and primary elimination via the liver. Thus, the observed low bioavailability was unexpected and suggested the possibility of poor absorption in this species. However, screening a number of vehicles did not result in any improvement over polyethylene glycol (PEG) 200 used in the initial study.[26]

Bile-duct cannulated (BDC) dog and portal/cephalic vein infusion studies were therefore carried out to better understand the reason for poor bioavailability. These studies revealed that **4** is well absorbed when dosed in PEG 200, with 78% of the total dose recovered in bile and urine as products of oxidative metabolism. Hepatic extraction, determined by comparing plasma AUCs during infusion via the portal or cephalic vein, was 80%. Therefore, despite the moderate clearance of **4** in dog, hepatic first-pass metabolism was the major factor limiting its bioavailability. As the dog was predicted to be most like human in pharmacokinetic profile based on the similar intrinsic clearance in these two species, improved dog pharmacokinetics (reduced clearance, increased bioavailability) was required to advance a compound into development. We therefore began a rational approach to identify molecules with this potential.

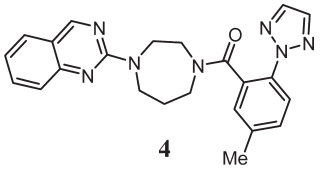

4

OX_1R: K_i = 1.2 nM; IC_{50} = 29 nM
OX_2R: K_i = 0.6 nM; IC_{50} = 27 nM

Figure 2. Previously reported diazepane-based DORA **4**.

In vitro metabolism studies of **4** in microsomal preparations indicated several sites of metabolism that we sought to eliminate or modify by synthetic modifications. A major metabolic pathway identified was oxidation of the tolyl methyl group on the 5-methyl-2-(triazolyl)-benzamide portion of the molecule to form the benzyl alcohol and further oxidation to the benzoic acid. Additionally, complex metabolic patterns were observed on the remainder of the molecule that indicated oxidation was occurring on both the core and the quinazoline heterocycle. Interestingly, when **4** was incubated in microsomal preparations fortified with semicarbazide, mass spectral adducts consistent with structure **4b** were identified (Scheme 1). Mechanistically, this is suggestive of oxidation at one of the four positions on the core adjacent to a nitrogen atom to form intermediate **4a**, followed by ring-opening to reveal an aldehyde, which is subsequently trapped by semicarbazide.[27] Taken as a whole, the metabolism data in hand suggested that removal of the benzylic methyl group, alteration of the heterocycle, and chemical modification of the core, especially blocking positions adjacent to the nitrogen atoms, were logical tactics to employ in an effort to improve pharmacokinetics in the diazepane series.

With this knowledge, we began an intensive synthetic investigation focused on identification of novel diazepane cores that had substitution at one or more carbon atoms. During this effort, we identified over 15 mono- or disubstituted diazepane cores that provided potent DORAs (K_i < 5 nM on both OX_1R and OX_2R). In general, substitution at positions 3 and 5 of the diazepane ring was not tolerated by the receptors, whereas substitution at positions 2, 6, and 7 was not only tolerated but often potency enhancing (Figure 3).[28]

With a large number of potent diazepane cores in hand, we combined these with the optimal triazolyl-benzamide substituent and various heterocycles to assemble a large number of potent DORAs for pharmacokinetic evaluation. Our expectation was that reduced IV clearance would predict improved bioavailability as a result of reduced metabolism, so we studied many compounds in parallel by dosing IV in the dog. Promising analogues were then followed up by PO dosing to determine bioavailability.[29] On the basis of the overall potency, ancillary, and pharmacokinetic profiles of analogues made with a methyl substituent at the 7-position of the diazepane core, these analogues were targeted for further investigation.

Surprisingly, a search of the literature revealed a dearth of practical synthetic strategies to access a simple orthogonally protected 7-methyldiazepane.[30] The most promising route

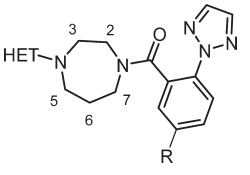

Figure 3. General scaffold for examining mono- and disubstituted diazepane cores.

Table 1. Pharmacokinetics of **4** in Rat and Dog

	IV[a]				PO[b]			
species	dose (mg/kg)	Cl (mL/min/kg)	Vd_{ss} (L/kg)	$T_{1/2}$ (h)	dose (mg/kg)	AUC (μM·h)	C_{max} (μM)	F (%)
rat	2	52.6	1.08	0.35	100	1.50	0.65	2
dog	0.5	11.6	0.86	1.28	3	1.81	1.44	16

[a] Vehicle = DMSO; n = 2 in rat, n = 3 in dog. [b] Rat: dosed as the HCl salt in 20% TPGS; n = 3; dog: dosed as free base in PEG 200, n = 2.

Scheme 1. Proposed Mechanism of Semicarbazide Trapping When **4** Is Incubated in Liver Microsomes Fortified with Semicarbazide

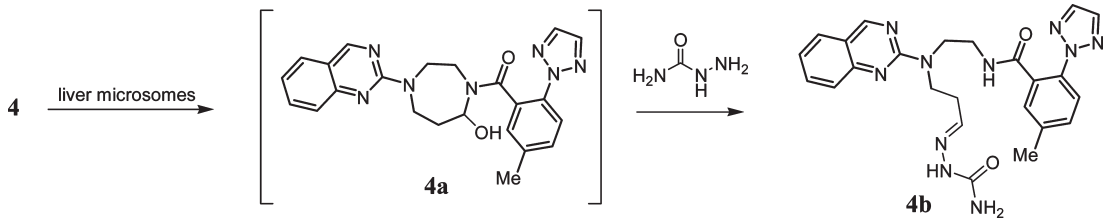

Scheme 2. Previously Reported Synthesis of the 7-Methyldiazepane Core[30b*a*]

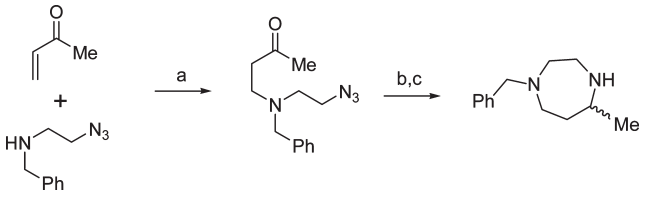

[a] Reagents and conditions: (a) Et_2O (70%); (b) PPh_3, Et_2O (72%); (c), LAH, Et_2O (91%).

Scheme 3. Synthesis of 7-Methyldiazepane DORA Analogues[a]

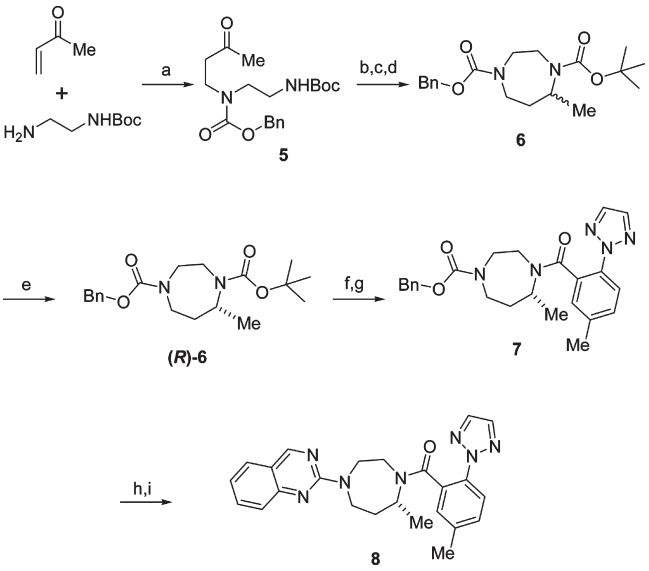

[a] Reagents and conditions: (a) Et_2O, then TEA and benzyl chloroformate; (b) $HCl_{(g)}$, EtOAc; (c) $NaBH(OAc)_3$, HOAc, CH_2Cl_2; (d) Boc_2O, TEA, CH_2Cl_2 (38% for 4 steps); (e) Chiralpak AD, 60% EtOH in hexanes (0.1% DEA as modifier), first isomer to elute is the desired (*R*)-isomer; (f) $HCl_{(g)}$, EtOAc; (g) 2-(2*H*-1,2,3-triazol-2-yl)-5-methylbenzoic acid, EDC, HOAT, NMM, DMF (87% for 2 steps); (h) H_2, $Pd(OH)_2$, MeOH/EtOAc; (i) 2-chloroquinazoline, K_2CO_3, DMF (75% for 2 steps).

involved conjugate addition of a 1,2-amino azide to methyl vinyl ketone, followed by an intramolecular aza-Wittig cyclization and subsequent reduction (Scheme 2).[30b] Although short and convergent, this route is unattractive for large scale synthesis because it necessitates the synthesis and use of a potentially explosive alkyl azide.[31]

As illustrated in Scheme 3, this route did, however, provide inspiration for a related strategy utilizing the commercially available *N*-Boc-1,2-diaminoethane as a surrogate for the azide. In our modified route, conjugate addition of the monoprotected diamine to methyl vinyl ketone followed by in situ trapping with benzyl chloroformate provides ketone **5**. Boc deprotection and subsequent intramolecular reductive amination with $NaBH(OAc)_3$ forms the diazepane ring. A Boc group is reinstalled to simplify purification, resulting in a 38% overall yield of **6** for the four steps from methyl vinyl ketone. Importantly, this chemistry can be readily carried out on large scale to provide access to quantities of **6** for analogue synthesis and in vivo evaluation of leading compounds.

Subsequent studies indicated that the (*R*)-antipode of analogues in this series had superior potency for the orexin receptors.[32] A chiral stationary phase HPLC resolution was therefore carried out on racemic **6** to provide the desired (*R*)-enantiomer as the first eluting isomer. To complete the synthesis of analogues in this series, Boc deprotection followed by amide coupling to 2-(2*H*-1,2,3-triazol-2-yl)-5-methylbenzoic acid provided **7** in excellent yield. Removal of the benzyl carbamate followed by reaction with 2-chloroquinazoline provided **8**, the 7-(*R*)-methyldiazepane analogue of **4** in 75% yield from **7**.

As illustrated in Table 2, **8** displayed excellent potency for OX_1R and OX_2R receptors in both binding and FLIPR assays, but a reduction in dog clearance did not lead to improved oral bioavailability relative to **4**. Synthesis of **9** which lacks the benzylic methyl group of **8** provided an analogue with similar IV clearance but with diminished potency on OX_1R as measured in the binding assay.[33] Installation of a fluorine atom at the 6-position of the quinazoline, a substitution we found to impart improved pharmacokinetics to a number of analogues in the diazepane series,[25b] provided **10** with improved potency, a further reduction in IV clearance, and favorable bioavailability of 37% in dog.

Similar to compound **4**, **10** is not a substrate for Pgp efflux (BA/AB = 0.6), has excellent passive permeability (38×10^{-6} cm/s), a plasma free fraction of ~3% in rat, and possesses a clean ancillary profile as determined by an MDS Pharma off-target screen. In vivo analysis in rat indicates **10** demonstrates reasonable rat pharmacokinetics with a clearance of 33 mL/min/kg and oral bioavailability of 47% when dosed at 10 mg/kg in 20% D-α-tocopheryl polyethylene glycol-100-succinate (TPGS)[34] and maintains a favorable brain/plasma ratio of 0.4−0.6 and a CSF/plasma ratio of 0.02−0.03.[35] Compound **10** possesses the overall profile we were seeking in a development compound, and it was therefore advanced into a rat sleep assay to assess its effects on sleep architecture.

The preclinical sleep laboratory at Merck makes use of radiotelemetric recording of electrocorticogram (ECoG) and electromyogram (EMG) signals to assess the time spent by animals in various states of arousal, including active wake, light sleep, REM sleep, and delta or slow wave sleep (SWS). Upon dosing **10** orally at 10 mg/kg/day to telemetry-implanted rats during their active phase (lights off), the amount of time spent in each state of arousal was measured and binned into 30 min intervals and compared to vehicle treated rats (Figure 4). Similar to the effects seen with compound **4**, **10**

Table 2. Profile of 7-(*R*)-Methyldiazepane Analogues **8**−**10**

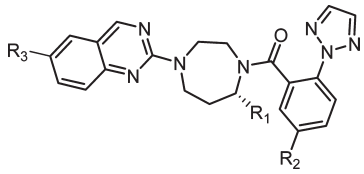

compd	R_1	R_2	R_3	OX_1R K_i, FLIPR[a] (nM)	OX_2R K_i, FLIPR[a] (nM)	dog Cl[b] (mL/min/kg)	dog F[c] (%)
4	H	Me	H	1.2, 29	0.59, 27	11.6	16
8	Me	Me	H	0.39, 30	0.36, 30	6.0	< 5
9	Me	H	H	6.2, 26	0.47, 18	6.4	ND
10	Me	H	F	1.8, 27	0.17, 27	5.2	37

[a] $n \geq 3$. [b] $n = 2$ in cassette (**8, 9**) or single (**4, 10**) mode. [c] $n = 2$ as a single in PEG 200.

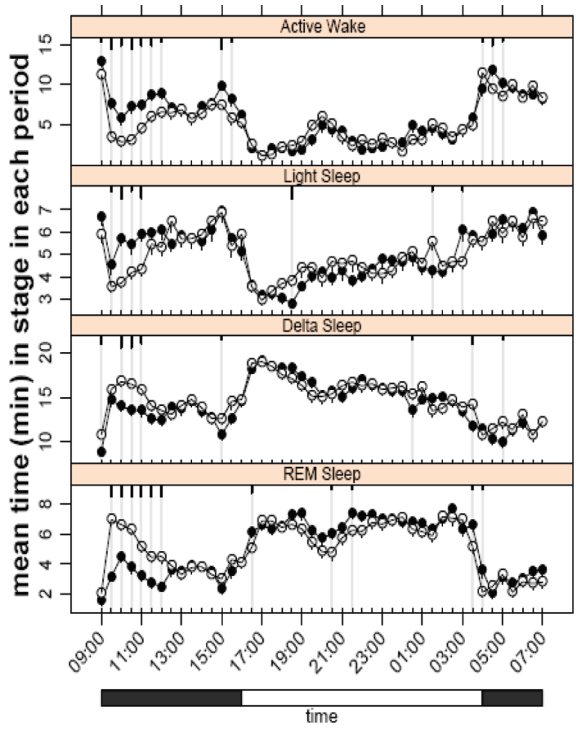

Figure 4. Effects of a 10 mg/kg dose of **10** on rat sleep. The duration of time spent in active wake, light sleep, delta sleep, and REM sleep in vehicle (closed circles) vs drug (open circles) treated animals following a 10 mg/kg po dose of **10** in 20% TPGS administered at 09:00. The open area in the bar above the abscissa designates lights on and the filled area designates lights off. Values are mean ± SEM. Vertical gray lines represent statistically significant differences from vehicle treatment as determined using mixed-model ANOVAs at each time point. Significance levels are indicated by length of tic marks (short < 0.5, medium < 0.01, long < 0.001).

produced a significant decrease in active wake with a concurrent increase in REM and delta sleep during the three to four hours following dosing. At approximately one hour post dose when the greatest effects on sleep are observed, the plasma exposure of **10** was ~1.0 μM, which leads to an estimated 20−30 nM in the CSF. Thus, compounds **4** and **10** induce favorable sleep effects in rats at comparable plasma exposures, as predicted based on their in vitro profile, but compound **10** works at a 10-fold lower dose (on a mg/kg basis) due to its improved bioavailability.

Excitement over the favorable attributes of **10** was tempered by the discovery that it undergoes bioactivation to form reactive electrophilic intermediates (reactive metabolites) that can be trapped with glutathione (GSH) when incubated in human or rat liver microsomes. It is generally accepted that reducing the potential for bioactivation of drug candidates during the lead optimization process is a prudent strategy to minimize potential risk for drug-induced idiosyncratic toxicity in humans.[36] We therefore next focused attention on reducing bioactivation of leading diazepanes.

To assess bioactivation potential, we employed an assay wherein test compounds were incubated in human liver microsomes fortified with GSH. Upon quenching the reaction, GSH-drug adducts were detected by ultra performance liquid chromatography−high resolution mass spectrometry (UPLC/HRMS).[37] The area under the peaks for all GSH-adducts was measured relative to an internal standard (IS), and the GSH-adduct/IS ratio was used as a semiquantitative measure of bioactivation potential.

In this assay, compound **10** had a GSH-adduct/IS ratio of 3.3. On the basis of mass spectral analysis of the GSH-adducts, we believed that the fluoroquinazoline ring was largely responsible for the bioactivation observed in **10**.[38] We therefore decided to hold constant the optimized 7-methyldiazepane core and triazolyl-benzamide while focusing on heterocycle replacements to maintain good pharmacokinetics and reduce bioactivation.

As illustrated in Table 3, replacing the fluoroquinazoline ring of **10** with a difluoroquinoxaline to provide **11** maintained favorable potency and IV clearance, but had little effect on the GSH-adduct/IS ratio. Believing a change from the 6,6-fused saturated ring system was required to reduce bioactivation, an analogue incorporating a 5,6,7,8-tetrahydroquinazoline ring was tested (**12**). Though potency remained excellent, dog clearance was adversely affected by this structural modification. Importantly, a significant improvement in the GSH-adduct/IS ratio was observed, indicating that progress toward reduced bioactivation was being made by alteration of the heterocycle.

Analysis of the historical dog IV data collected on the program to this point identified benzoxazole-containing diazepanes as generally having reduced clearance values relative to other heterocycles tested. Installation of an unsubstituted benzoxazole to provide **13** resulted in an analogue with the lowest plasma clearance in dog observed to date for a diazepane DORA (2.4 mL/min/kg). However, despite inclusion of the potency-enhancing methyl group on the benzamide,[33] **13** suffered a nearly 20-fold loss in OX_2R binding potency relative to **10**. From previous SAR knowledge dating back to the HTS hit that led to the discovery of the diazepane series, it was known that addition of lipophilic groups on benzoxazoles and

Table 3. Profile of 7-(*R*)-Methyldiazepane Analogues

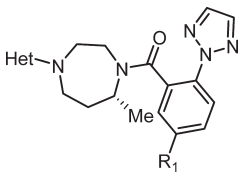

Compd	Het	R_1	OX_1R K_i, FLIPR [a] (nM)	OX_2R K_i, FLIPR [a] (nM)	Dog Cl [b] (ml/min/kg)	Dog F [c] (%)	GSH/IS ratio [d]
10	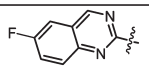	H	1.8, 27	0.17, 27	5.2	37	3.3
11	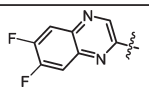	H	1.8, 28	0.25, 32	4.9	15	3.7
12	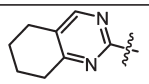	H	0.78, 24	0.28, 28	9.2	ND	0.7
13	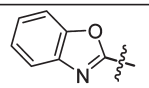	Me	4.1, 24	3.2, 57	2.4	ND	ND
3	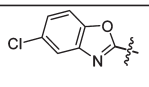	Me	0.55, 50	0.35, 56	4.0	56	0.1

[a] $n \geq 3$. [b] $n = 2$ in cassette (**12**, **13**) or single (**10**, **11**, **3**) mode. [c] $n = 2$ as a single in PEG 200. [d] See Experimental Section for a description of how this number is calculated.

benzothiazoles provided significant potency increases. Indeed, installation of a chlorine at the 5-position of the benzoxazole provided **3** with excellent potency and pharmacokinetics as well as minimal GSH-adduct formation (GSH-adduct/IS ratio = 0.1). We therefore decided to further characterize **3** for its potential as a development candidate.[39]

Like its predecessors, **3** possesses a favorable profile for a CNS-penetrant drug. It is not a substrate for Pgp efflux (BA/AB = 0.8), has excellent passive permeability (37×10^{-6} cm/s), and possesses a clean ancillary profile (> 10000-fold selectivity for OX_2R) as determined by an MDS Pharma off-target screen of 170 enzymes, receptors, and ion channels. Because of the added lipophilicity introduced by the chlorobenzoxazole relative to the fluoroquinazoline (the LogP increased from 3.0 in **10** to 3.6 for **3**), protein binding increased to ~99% in both rat and human plasma. DORA **3** has a brain/plasma ratio of ~1 in the rat, and its CSF concentration is well reflected by unbound plasma concentration, suggesting a lack of concentration gradient between plasma and brain.[40]

When studied in telemetry-implanted rats, **3** induced significant changes in sleep behavior at 30 mg/kg where, as expected, significant increases in REM and delta sleep are observed with a corresponding decrease in active wake (Figure 5).[41] In this study, the plasma exposure of **3** reached a C_{max} of 2.1 μM, which leads to an estimated 21 nM in the CSF.

Along with the rat sleep assay, another powerful tool that aided lead optimization efforts was an ex vivo occupancy assay designed to measure orexin receptor binding directly in the rat brain. Because of low levels of endogenous orexin receptor expression, we developed a transgenic line of rats engineered to overexpress the human OX_2R ubiquitously in the brain at relatively high density (12−14 nM).[41] This assay allowed us to determine receptor occupancy in the rat brain following peripheral administration of antagonists. Following a 30 min IV infusion of **3** over a concentration range of 0.1−2.0 mpk, we found that a 1.34 mg/kg dose was required to occupy 90% of the orexin receptors (Occ_{90}), corresponding to exposures of 1070 nM in plasma, 1180 nM in brain, and 13 nM in the CSF (Figure 6). This suggests that in the rat sleep study at 30 mg/kg/day, **3** achieved greater than 90% receptor occupancy.

As illustrated in Table 4, **3** has high clearance in rat but low to moderate clearance in dog, with a short terminal half-life of 0.6 and 3.3 h, respectively. Compound **3** also has good bioavailability in dog with a rapid T_{max} but lower bioavailability in rat. Investigation of **3** in BDC rat and dog studies following IV administration of ^{14}C-labeled drug not unexpectedly identified oxidation of the tolyl methyl group to the corresponding benzyl alcohol (**14**) as a major route of metabolism (Scheme 4). Further oxidation to the carboxylic acid **15** was also observed, as was oxidation of the methyl group on the core (**16**) and oxidation on the left-hand portion of the molecule (**17**).[42] Further conversion to the corresponding glucuronides was also observed. In rat, dog, and human liver microsomes, these same oxidative metabolites were observed, with rat microsomes displaying the highest rate of metabolism relative to dog and human. On the basis of the in vitro and in vivo data, and an assumption that oxidative metabolism will be the primary mode of elimination, **3** was predicted to be a

low to moderate clearance compound with good bioavailability and a rapid onset of action in humans.

Compound **3** is a semicrystalline solid with good thermal- and pH-dependent stability and modest aqueous solubility.

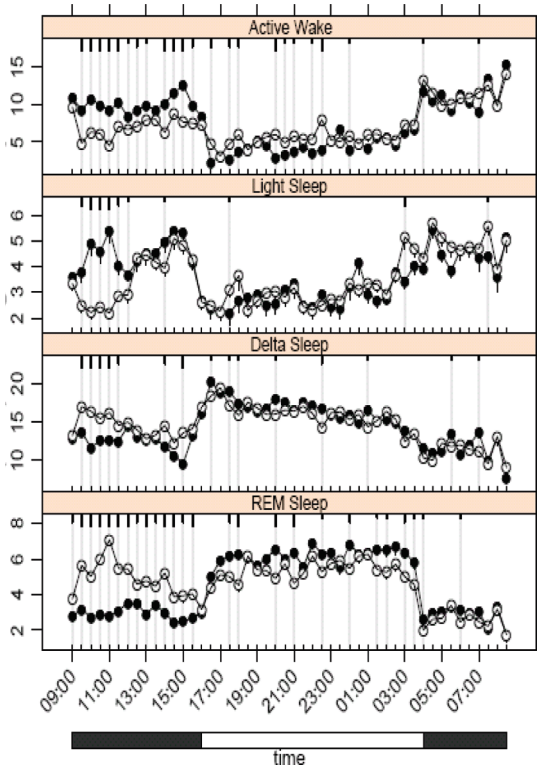

Figure 5. Effects of a 30 mg/kg dose of **3** on rat sleep. The duration of time spent in active wake, light sleep, delta sleep, and REM sleep in vehicle (closed circles) vs drug (open circles) treated animals following a 30 mg/kg po dose of **3** in 20% TPGS administered at 09:00. The open area in the bar above the abscissa designates lights on and the filled area designates lights off. Values are mean ± SEM. Vertical gray lines represent statistically significant differences from vehicle treatment as determined using mixed-model ANOVAs at each time point. Significance levels are indicated by length of tic marks (short < 0.5, medium < 0.01, long < 0.001).

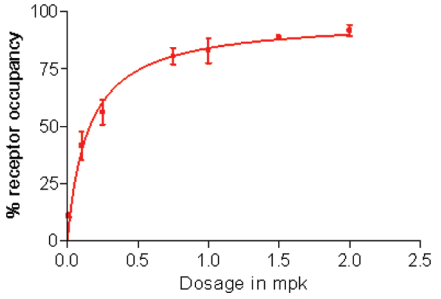

Figure 6. Plot of occupancy versus dose for compound **3** in transgenic rats. Similar plots of occupancy versus concentration of **3** in plasma, brain, or CSF can be generated.

It was not genotoxic and was well-tolerated in preclinical pharmacology and toxicity studies. There were no cardiovascular effects in dogs, and neurobehavioral changes in mice and rats were generally limited to transient decreases in locomotor activity that were consistent with the intended mechanism of action. Results from one-month general toxicity studies in rats and dogs supported the safety and tolerability of **3** for short-term testing in humans. On the basis of the overall profile of **3**, it was approved for development and entered phase I clinical trials in 2007. In late 2009, a phase III clinical trial was initiated to study the long-term safety and efficacy of **3** for the treatment of primary insomnia.[23] Additional preclinical as well as clinical results will be reported in due course.

In conclusion, we have described how a diazepane lead compound was advanced to provide a potent, brain-penetrant dual orexin receptor antagonist for the treatment of insomnia. Efforts to understand the cause of the poor pharmacokinetics of **4** led to a rational search for chemical modifications that reduced metabolism. Identification of the favorable 7-methyl substituent on the diazepane core resulted in compound **10** with good potency, improved pharmacokinetics, and excellent in vivo efficacy. An in vitro assay to assess bioactivation, in concert with a mechanistic hypothesis as to the site of bioactivation, led to replacement of the fluoroquinazoline ring of **10** with a chlorobenzoxazole to provide **3**, a potent dual orexin receptor antagonist that is currently being tested in phase III studies for the treatment of primary insomnia.

Experimental Section

A. Biology. All animal studies were performed according to the NIH Guide for the Care and Use of Laboratory Animals, and experimental protocols were reviewed by the Merck Animal Care and Use Committee.

Radioligand Binding Assay. Membranes were prepared from expressed human orexin 2 receptor (hOX_2R) and the Ile408-Val variant of orexin 1 receptor (hOX_1R) in CHO cells according to the method described by Kunapuli et al.[43] Confluent CHO/OX_2R and CHO/OX_1R cells were dissociated from flasks with PBS/1 mM EDTA and centrifuged at 1000*g* for 10 min. The cell pellets were homogenized with a Polytron in ice-cold 20 mM Hepes, 1 mM EDTA, at pH 7.4, and centrifuged at 20000*g* for 20 min at 4 °C. This process was repeated twice. The final membrane pellet was resuspended at 5 mg of membrane protein/mL in assay buffer (20 mM Hepes, 125 mM NaCl, 5 mM KCl, pH 7.4). Bovine serum albumin was added to achieve a final concentration of 1% and aliquots stored at −80 °C. Radioligand binding assays were performed utilizing an automated Tecan Liquid handling system and Packard Unifilter-96 as described by Mosser et al.[44] Assays were performed at room temperature in 96-well microtiter plates with a final assay volume of 1.0 mL in 20 mM Hepes buffer (pH 7.4) containing 125 nM NaCl and 5 mM KCl. Solutions of test compounds were prepared in DMSO and serially diluted with DMSO to yield 20 μL of each of 10 solutions differing by 3-fold in concentration. Nonspecific binding (NSB) is determined using a high-affinity ligand (1 μM final concentration) and total binding (TB) is determined by using DMSO (2% final concentrations). A solution of receptor (30 pM final, typically 2−10 μg membranes),

Table 4. Pharmacokinetic Parameters of **3** in Rat and Dog

	IV[a]				PO[b]				
species	dose (mg/kg)	Cl (mL/min/kg)	Vd_{ss} (L/kg)	$T_{1/2}$ (h)	dose (mg/kg)	AUC (μM·h)	C_{max} (μM)	T_{max} (h)	*F* (%)
rat	2	44	2.6	0.6	10	1.7	0.48	0.5	19
dog	0.5	4.0	0.8	3.3	3	16.9	3.2	0.5	56

[a] Vehicle = DMSO; $n = 3$. [b] PEG 200, $n = 3$.

Scheme 4. Oxidative Metabolites of **3** Identified from a BDC Rat Study

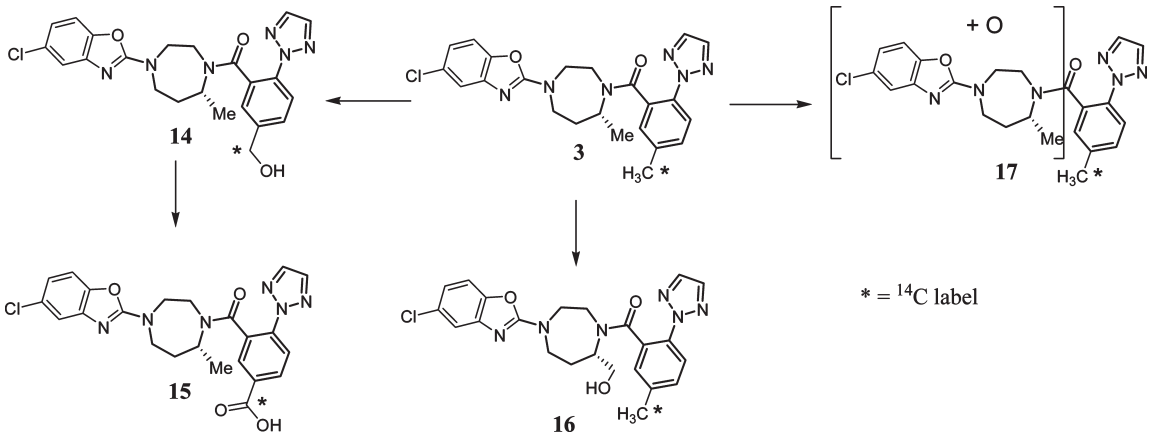

and tritiated ligands (~80 Ci/mmole) were added to the test compounds. For the OX_2R receptor, 0.15 nM of compound **18** (K_D = 0.3 nM) was used. For the OX_1R receptor, 0.7 nM of compound **19** (K_D = 3 nM) was used. The OX_1R assay was also performed with equivalent results using compound **20** at a concentration of 0.03 nM (K_D = 0.03 nM); however, in this case 920 μL of membranes was added first to the compounds followed by the addition of 60 μL of the hot ligand. After 3 h of incubation at room temperature (20 h for compound **20**), samples were filtered through Packard GF/B filters (presoaked in 0.2% PEI, polyethyleninine Sigma P-3143) and washed five times with 1 mL of cold 20 mM Hepes buffer (pH 7.4) per wash. After vacuum drying of the filter plates, 50 μL of Packard Microscint-20 was added and bound radioactivity (CPM bound) determined in a Packard TopCount.

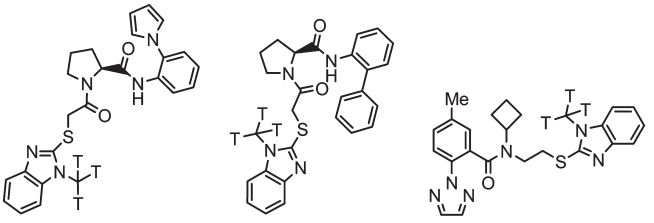

18 **9** **20**

Dose-inhibition profiles for each compound were characterized by fitting the data to a four-parameter equation using an Excel based fitting program as previously described by Mosser et al.[44] The apparent inhibition constant ($\boldsymbol{K_I}$, $K_I = 10^{-\mathbf{pK_I}}$), the maximum inhibition at the low plateau relative to "100% inhibition control" ($\boldsymbol{I_{max}}$; e.g. 1 ≥ same as this control), the minimum inhibition at the high plateau relative to the "0% inhibition control" ($\boldsymbol{I_{min}}$, e.g. 0 ≥ same as the no drug control) and the Hill slope (***n*H**) are determined by a weighted nonlinear least-squares fitting of the raw experimental observations (CPM Bound) as a function of dose ([Drug]) according to the equation below:

$$\mathrm{CPMBound} = \frac{(\mathrm{TB}-\mathrm{NSB})(I_{max}-I_{min})}{1+\left[\frac{[\mathrm{Drug}]}{\left(10^{-\mathrm{p}K_I}\left(1+\frac{[\mathrm{Radiolabel}]}{K_D}\right)\right)}\right]^{n\mathrm{H}}} + \mathrm{NSB} + (\mathrm{TB}-\mathrm{NSB})(1-I_{max}) \quad (1)$$

The median signal of the "0% inhibition controls" (TB) and the median signal of the "100% inhibition controls" (NSB) are constants in eq 1 that are determined from the controls located in columns 1 and 12 of each assay plate. The concentration of radioligand in eq 1 ([Radiolabel]) is calculated for each run based on the ligand specific radioactivity and the measured CPM of an aliquot of the assay solution. The apparent dissociation constant of the radioligand for its receptor (K_D) in eq 1, and the receptor concentration (B_{max}) is determined by a hot saturation experiment.

FLIPR Assay. For intracellular calcium measurements, Chinese hamster ovary (CHO) cells expressing the Ile408-Val variant of the orexin 1 receptor or the human orexin 2 receptor, were grown in Iscove's modified DMEM containing 2 mM L-glutamine, 0.5 g/mL G418, 1% hypoxanthine-thymidine supplement, 100 U/mL penicillin, 100 ug/mL streptomycin, and 10% heat-inactivated fetal calf serum. The cells were seeded at 20000 cells/well into Becton-Dickinson black 384-well clear bottom sterile plates coated with poly-D-lysine. All reagents were from GIBCO-Invitrogen Corp. The seeded plates were incubated overnight at 37 °C and 6% CO_2. Ala-6,12 human orexin-A as the agonist was prepared as a 0.5 mM stock solution in 1% bovine serum albumin (BSA) and diluted in assay buffer (HBSS containing 20 mM HEPES and 2.5 mM probenecid, pH 7.4) for use in the assay at a final concentration of 0.3−2 nM. Test compounds were prepared as 10 mM stock solution in DMSO, then diluted and pipetted in 384-well plates, first in DMSO, then assay buffer. On the day of the assay, cells were washed three times with 100 μL assay buffer and then incubated for 60 min (37 °C, 6% CO_2) in 60 μL of assay buffer containing 1 μM Fluo-4AM ester, 0.02% pluronic acid, and 1% BSA. The dye loading solution was then aspirated and cells washed three times with 100 μL of assay buffer. Then 30 μL of that same buffer is left in each well. Within the fluorescent imaging plate reader (Molecular Devices), test compounds were added to the plate in a volume of 15 μL, incubated for 5 min, and finally 15 μL of agonist was added. Fluorescence was measured for each well at 1 s intervals for 1 min and at 6 s intervals for 4 min, and the height of each fluorescence peak was compared to the height of the fluorescence peak induced by 0.3−2 nM Ala-6,12 orexin-A with buffer in place of antagonist. For each antagonist, the IC_{50} value (the concentration of compound needed to inhibit 50% of the agonist response) was determined.

Rat Sleep Assay. Adult male Sprague−Dawley rats (450−600 g; Taconic Farms, Germantown, NY) were subcutaneously implanted with telemetric physiologic monitors (model F50-EEE or 4ET SI; Data Sciences International, Arden Hills, MN) that were used to simultaneously record both the electrocorticogram (ECoG) and electromyogram (EMG) activities of the rat. For placement of the 4ET SI, animals were anesthetized with isoflurane and electrodes for recording ECoG signals and EMG signals were placed. Position of the wires are based on the following coordinates. Channel 1 wire. From Lambda AP +2,

ML +2 −2. Channel 2 wires From BREGMA AP +1.5 ML +3.2 (hole 1) AP −10.5 (hole2). Channel 3 wires From BREGMA AP −3.0 ML +1.5, −3.5. EMG lead placement was in neck muscle. An incision was made ∼3−5 cm in length midline on the dorsal thorax to form a pocket on the left and right side of midline, and the telemetry module was placed with a saddlebag placement method. The animals were given a single dose of antibiotic (gentomycin, 5.8 mg/kg) and an analgesic (buprenorphine, 0.1 mL) within 3 h following surgery. The animals were allowed to recover from surgery for at least two weeks prior to recording. Throughout these experiments, animals were housed individually in plastic cages (19 in. × $10^{1}/_{2}$ in. × 8 in.; Lab Products, Seaford, DE) and were provided water and food ad libitum. Lights were on a 12 h light: 12 h dark cycle with lights off at 4:00 a.m. and on at 4:00 p.m. ECoG and EMG signals were collected simultaneously from all animals using Dataquest ART software system (Data Sciences International, Arden Hills, MN), digitally sampled at 500 Hz, and stored on a PC for off-line analysis.

The hydrochloride salt of compound **10** (458 mg) was dissolved in 70.2 mL of a 20% aqueous solution of TPGS (obtained from Eastman Chemical Company) and administered by oral gavage at 10 mpk of the free-base equivalent to four rats, 5 h into their active period (09:00 or ZT 17:00). For **3**, the free-base (1.27 g) was suspended in 70.2 mL of a 20% aqueous solution of TPGS and dosed as above. Recordings were started just prior to compound administration and were collected for 23 h. The experiments were based on a standard crossover design with two animals receiving compound for one week and the complementary group receiving vehicle, followed by a week of reversed administration. All animals were exposed to two days administration of orally gavaged vehicle prior to initiation of experimental drug administration to allow for habituation. For baseline sleep measurements, continuous recordings were collected for two days to get average sleep behaviors for each animal over contiguous days prior to drug and vehicle administration. During the drug administration studies, recordings were collected each day prior to, during, and following drug administration. Recordings were begun prior to compound administration so that the exact time of administration was recorded within the raw data file as artifactual noise which was caused by removing the implanted transmitter from the receptive field of the receiver during administration. This information allowed a direct measure of drug/vehicle administration time during offline analysis and was not included in the data analysis. Following the completion of data collection, all data were scored with automated sleep stage analysis software, Somnologica (Embla, Broomfield, CO). Assignment of sleep stages was made in general accord with those described by J. M. Monti's group.[45] Sleep/wake stages were assigned based upon a combination of level of movement within the field of the radio frequency receiver over which individually housed rats were caged, EMG activity, and ECoG frequencies over 10 s epochs. Active wake was assigned to the epoch when movement of the animal was detected over the receiver or when there was an active EMG signal over the epoch and the ECoG frequencies consisted of low-voltage high frequency activity. An epoch was scored as light sleep when there was no movement activity, the EMG was moderately activ,e and the ECoG consisted of either theta or theta activity mixed with less than 50% of the epoch showing delta activity. Delta sleep was scored when there was no gross movement, reduced EMG activity, and the ECoG consisted of more than 50% delta wave activity (i.e., 0.5 to 4 Hz). Rapid eye movement (REM) sleep was scored when there was no movement or EMG activity and the ECoG consisted of primarily theta activity. Results of staging were grouped into 30 min periods following drug administration and the number of entries into each stage and the duration of minutes spent in each stage were calculated. The results for all four animals were averaged by treatment, or vehicle, over seven administration nights and the results were statistically compared based upon a mixed ANOVA analysis.

Bioactivation Assay. Human liver microsomes (pooled, BD Gentest) were preincubated at 1 mg/mL protein in 100 mM potassium phosphate buffer (pH 7.4) with 10 μM test compound, 1 mM $MgCl_2$, 1 mM EDTA, 5 mM glutathione, and 1 mM NADPH for 60 min at 37 °C. The reactions were terminated with 25% acetonitrile containing 0.15 μM labetalol (internal standard). The samples were vortex-mixed and centrifuged at 14000 rpm for 10 min. The supernatant from each sample was transferred to an HPLC vial for HRMS analysis.

UPLC-high resolution mass spectrometry (HRMS) was used to identify the GSH-derived adducts. The system consisted of a Waters Acquity sample manager and two Waters Acquity UPLC pumps. HRMS was performed using a Waters Q-TOF Xevo mass spectrometer. Separation was achieved using a Phenomenex Synergi 2.5 μm MAX-RP 100 Å column (50 mm × 2 mm) heated to 60 °C. The mobile phase consisted of water with 0.1% formic acid (solvent A) and acetonitrile with 0.1% formic acid (solvent B) at a flow rate of 0.5 mL/min. The gradient began with 5% solvent B for the first minute, followed by a linear increase to 15% solvent B over the next 0.5 min. Solvent B was then increased to 50% over the next 11.5 min followed by a further increase to 90% over 2 min. The column was then washed with 95% solvent B for 1.5 min. At the end of each run, the column was re-equilibrated for 5 min at the initial conditions. Mass spectral analyses were carried out using electrospray ionization in positive ion mode. The ESI capillary voltage was set at 1.5 kV, and the source and desolvation temperatures were set at 100 and 600 °C, respectively. The mass scan range was 150 to 1000 amu with 0.25 s/scan. The lock mass of 588.8691 amu was used with a frequency of one scan per 5 scans. The relative amount of GSH adducts formed with each test compound was estimated using peak area ratios. The areas obtained from the mass spectral peaks associated with GSH-derived adducts were divided by the area of the internal standard, labetalol.

Ex Vivo Occupancy Assay. Transgenic rats expressing human OX_2R were dosed intravenously by infusion over a 30 min period or orally with **3** at doses of 0.1−2.0 mg/kg in 25% hydroxypropyl-β-cyclodextrin and then sacrificed. Samples of brain were quickly removed and frozen for use in the ex vivo occupancy assay, while a second set of tissue samples, a plasma sample, and CSF were frozen for LCMS determination of drug levels. For the ex vivo assay, approximately 60 mg of cord or brain was homogenized in 67 volumes of ice-cold assay buffer (20 mM HEPES, 120 mM NaCl, 5 mM KCl, pH7.4) and centrifuged at 21000*g* for 1 min. The pellets were resuspended in ice-cold buffer at a concentration of 10 mg tissue/mL and 100 μL aliquots were rapidly distributed to tubes with 0.5 mL rof oom temperature buffer containing 200 pM compound **A**. At 2, 4, 6, 8, 10, 12, and 15 min following membrane addition, incubations were terminated by filtration of three tubes over glass fiber filters. A parallel set of incubations performed in the presence of 1 μM of an unlabeled, potent DORA (OX_2R K_i = 1.0 nM) was used to determine nonspecific radioligand binding at each time point. Radioactivity on the filters was determined by liquid scintillation counting and compound **A** rates of association were determined by linear regression. Receptor occupancy in a drug treated animal is calculated as: % occupancy = $(1 - (\text{slope}_{\text{drug}}/\text{slope}_{\text{vehicle}})) \times 100$. The concentrations of drug required to achieve 90% receptor occupancy were derived by nonlinear curve fitting using Prism software.

B. Chemistry. All solvents used were commercially available "anhydrous" grade, and reagents were utilized without purification unless otherwise noted. Nonaqueous reactions were carried out in oven- or heat gun-dried glassware under a nitrogen atmosphere. Magnetic stirring was used to agitate the reactions and they were monitored for completion by either TLC (silica gel 60, Merck KGaA) or LC/MS. A SmithCreator microwave

from Personal Chemistry was used for microwave heating, and a CombiFlash system utilizing RediSep cartridges by Teledyne Isco was utilized for silica gel chromatography with fraction collection at 254 nm. Reverse phase HPLC purification was carried out on a Waters HPLC (XBridge Prep C-18 5 μM 19 mm × 150 mm column) utilizing a gradient of 0.1% TFA in water/acetonitrile with sample collection triggered by photodiode array detection. The reported yields are for isolated compounds of ≥95% purity, unless otherwise noted, and were not extensively optimized. Purity analysis was carried out by HPLC with a Waters 2690 separations module equipped with a YMC Pro 50 mm × 3 mm I.D. C-18 column interfaced with a Waters Micromass ZMD spectrometer utilizing a gradient of 0.05% TFA in water/acetonitrile with UV detection at 215 and 254 nm. ^{1}H and ^{13}C NMR spectra were recorded on a Varian INOVA 400, 500, or 600 MHz spectrometer, and all chemical shifts are referenced to an internal standard of tetramethylsilane or the $CDCl_3$ solvent peak, respectively. High resolving power accurate mass measurement electrospray (ES) and atmospheric pressure chemical ionization (APCI) mass spectral data were acquired by use of a Bruker Daltonics 7T Fourier transform ion cyclotron resonance mass spectrometer (FT-ICR MS). Optical rotations were determined at 23 °C on a Perkin-Elmer 241 spectrometer in the solvents and at the concentrations specified.

As we have recently described, 1,4-disubstituted diazepane orexin receptor antagonists exhibit unusual conformations in solution and exist in multiple conformations as a result of hindered rotations that are slow on the NMR time-scale.[25a] In the case of compound **4**, we attributed the four conformations to *cis*−*trans* amide isomerization and hindered rotation about the exocyclic C−N bond between the core and the quinazoline. In a similar vein, the proton spectra of compounds **3** and **7**−**13** consist of broad, overlapping multiplets precluding a detailed coupling constant analysis, and we feel that pictorial reproductions of the NMR spectra are more informative for comparative purposes; thus, NMR resonances of final compounds will not be listed in numerical format. Instead, we include reproductions of the ^{1}H and ^{13}C NMR spectra at 25 °C of all final compounds in the Supporting Information, as well as the synthetic procedures for preparation of **8**−**13**. For compound **3** only, ^{1}H and ^{13}C chemical shifts assigned from the analysis of COSY, HSQC, and HMBC spectra will be presented herein.

[(7*R*)-4-(5-Chloro-1,3-benzoxazol-2-yl)-7-methyl-1,4-diazepan-1-yl][5-methyl-2-(2*H*-1,2,3-triazol-2-yl)phenyl]methanone (3). To a solution of **7** (29.5 g, 68.3 mmol) in 300 mL of EtOAc and 200 mL of MeOH under nitrogen was added 2.4 g of 20% $Pd(OH)_2$ on carbon. The reaction was stirred for 48 h at room temperature under a balloon of H_2, then filtered through a pad of celite with the aid of additional MeOH and concentrated to provide 21.0 g (100%) of the secondary amine as a white foam. This material was dissolved in 250 mL of DMF, and to the solution was added triethylamine (29.3 mL, 210 mmol) and 2,5-dichloro-1,3-benzoxazole[46] (13.2 g, 70.1 mmol). After stirring for 2 h at 75 °C, the reaction was partitioned between EtOAc and saturated aqueous $NaHCO_3$, the layers were separated, and the organic layer was washed with water, brine, dried over $MgSO_4$, filtered, and concentrated by rotary evaporation. The residue was purified by column chromatography with a gradient of 0−100% EtOAc in hexanes to provide a colorless foam. This material was stirred in a solution of 150 mL of EtOAc and 300 mL of hexanes overnight, filtered through a Büchner funnel, and the solids were collected to provide 29.1 g (92% from **7**) of **3** as a white solid. HRMS calcd for $C_{23}H_{23}ClN_6O_2$ (M + H): 451.1644; found 451.1631. $[\alpha]_D = -24.8$ ($c = 1.0$, chloroform).

Compound **3** exists as a mixture of four rotameric components in chemical exchange in DMSO-d_6 at room temperature (48:24:18:10). ^{1}H and ^{13}C chemical shifts of the two most populated rotamers were assigned from the analysis of COSY, HSQC, and HMBC spectra acquired on a sample dissolved in DMSO-d_6 at 25 °C. See the Supporting Information for reproductions of the ^{1}H and ^{13}C NMR spectra at 25 °C in $CDCl_3$.

Rotamer 1: (48% of total) ^{1}H NMR (599.458 MHz, DMSO-d_6, 25 °C) δ 7.90 (2H), 7.82 (1H), 7.44 (2H), 7.35 (1H), 7.32 (1H), 7.04 (1H), 4.23 (1H), 4.06 (1H), 3.98 (1H), 3.77 (1H), 3.62 (1H), 3.53 (1H), 3.32 (1H), 2.41 (3H), 2.04 (1H), 1.64 (1H), 1.15 (3H). ^{13}C NMR (150.742 MHz, DMSO-d_6, 25 °C) δ 167.9, 162.9, 147.4, 147.1, 144.9, 137.9, 135.7, 133.4, 130.3, 128.0, 127.7, 122.1, 119.6, 114.9, 109.6 51.6, 46.3, 43.0, 39.8, 34.8, 20.2, 18.9.

Rotamer 2: (24% of total) ^{1}H NMR (599.458 MHz, DMSO-d_6, 25 °C). 8.04 (2H), 7.79 (1H), 7.42 (1H), 7.38 (1H), 7.31 (1H), 7.24 (1H), 7.02 (1H), 4.64 (1H), 4.25 (1H), 4.00 (1H), 3.94 (1H), 3.73 (1H), 3.58 (1H), 3.22 (1H), 2.34 (3H), 2.20 (1H), 1.77 (1H) 1.13 (3H). ^{13}C NMR (150.742 MHz, DMSO-d_6, 25 °C) δ 168.3, 162.6, 147.3, 147.1, 144.7, 138.2, 135.8, 133.0, 130.2, 128.1, 127.9, 121.9, 119, 114.9, 109.6, 47.7, 46.5, 44.4, 38.4, 32.7, 20.1, 16.1.

***tert*-Butyl {2-[(3-Oxobutyl)amino]ethyl}carbamate, Carbobenzyloxy-Protected (5).** To a solution of *tert*-butyl *N*-(2-aminoethyl)carbamate (39.4 mL, 250 mmol) in 500 mL of Et_2O was added methyl vinyl ketone (20.5 mL, 250 mmol) dropwise. After stirring 18 h, the reaction was cooled to 0 °C and triethylamine (45.2 mL, 325 mmol) was added, followed by dropwise addition of benzyl chloroformate (39.2 mL, 250 mmol). The reaction was allowed to warm slowly to room temperature and then stirred 48 h before being partitioned between EtOAc and 10% aqueous citric acid in a separatory funnel. After separation, the aqueous layer was extracted again with EtOAc, the combined organic layers were washed with saturated aqueous $NaHCO_3$, then brine, dried over Na_2SO_4, and concentrated by rotary evaporation to provide 71.3 g of crude **5** as pale yellowish−brown oil that was carried into the next step without further purification.

1-Benzyl 4-*tert*-Butyl 5-Methyl-1,4-diazepane-1,4-dicarboxylate (6). HCl gas was bubbled through a solution of 71.3 g crude **6** in 500 mL of EtOAc until the reaction was warm to the touch, the flask was capped, and stirred for 2 h at room temperature. The volatiles were removed by rotary evaporation, the residue was dissolved in 1 M HCl and washed twice with Et_2O. The aqueous layer was carefully basified with NaOH and extracted three times with 2:1 $CHCl_3$/EtOH. The combined organic phases were washed with a minimum amount of brine and concentrated by rotary evaporation. The residue was dissolved in CH_2Cl_2, filtered, and concentrated to provide 32.9 g of a brown oil. This material was dissolved in 400 mL of CH_2Cl_2 and treated with 10 mL of acetic acid. After stirring 2 h at room temperature, sodium triacetoxyborohydride (39.6 g, 187 mmol) was added and the reaction was stirred 48 h at room temperature. Most of the solvent was removed by rotary evaporation, and the residue was dumped into saturated aqueous $NaHCO_3$ and extracted three times with 2:1 $CHCl_3$/EtOH. The combined organic phases were washed with a minimum amount of brine and concentrated by rotary evaporation. The residue was dissolved in CH_2Cl_2, filtered, and concentrated to provide 32.3 g of a brown oil. This material was dissolved in 200 mL of CH_2Cl_2 and treated with triethylamine (26.3 g, 260 mmol) and Boc_2O (34.1 g, 156 mmol). After stirring overnight at room temperature, the reaction was diluted with additional CH_2Cl_2 and washed sequentially with 10% aqueous citric acid, saturated aqueous $NaHCO_3$, water, dried over Na_2SO_4, and concentrated by rotary evaporation. The residue was purified by column chromatography with a gradient of 0 to 30% EtOAc in hexanes to provide 33.1 g (38% from methyl vinyl ketone) of **6** as a colorless oil. ^{1}H NMR (500 MHz, $CDCl_3$) δ 7.4−7.3 (m, 5H), 5.1 (s, 2H), 4.25 (m, 0.5H), 4.0−3.6 (m, 4H), 3.3−2.9 (m, 3.5H), 2.1 (m, 1H), 2.55 (s, 9H), 1.1 (d, $J = 6.6$ Hz, 3H) ppm. LRMS = 249.1 (M + H − Boc).

1-Benzyl 4-*tert*-Butyl (5*R*)-5-Methyl-1,4-diazepane-1,4-dicarboxylate [(*R*)-6]. Resolution of the enatiomers of **6** was carried out chromatographically using a Chiralpak AD 10 cm × 50 cm column with 60% EtOH in hexanes (containing 0.1% diethylamine as a modifier) at 175 mL/min. Resolution of 17.4 g of **6** in

three equal injections provided 8.2 g (47%, 95% of theoretical) of (***R***)-**6** as the first eluting enatiomer. Analytical HPLC analysis carried out on a 46 mm × 250 mm Chiralpak AD column with the same eluent as above at a flow rate of 1 mL/min indicated that (***R***)-**6** was of >98% ee. ^{1}H NMR (500 MHz, $CDCl_3$) δ 7.4−7.3 (m, 5H), 5.1 (s, 2H), 4.25 (m, 0.5H), 4.0−3.6 (m, 4H), 3.3−2.9 (m, 3.5H), 2.1 (m, 1H), 2.55 (s, 9H), 1.1 (d, J = 6.6 Hz, 3H) ppm. LRMS = 249.1 (M + H − Boc). $[\alpha]_D$ = −24.3 (c = 1.0, chloroform).

2-(2*H*-1,2,3-Triazol-2-yl)-5-methylbenzoic Acid. A solution of 2-iodo-5-methylbenzoic acid (4.0 g, 15.3 mmol) in DMF (10 mL) was treated with 1,2,3-triazole (2.1 g, 30.5 mmol), Cs_2CO_3 (9.95 g, 30.5 mmol), CuI (0.145 g, 0.76 mmol), and *trans*-*N*,*N*′-dimethylcyclohexane-1,2-diamine (0.43 g, 3.05 mmol). The mixture was heated at 120 °C for 10 min in a microwave reactor. The reaction was cooled to room temperature, diluted with water, and washed with EtOAc. The aqueous phase was acidified with 1N HCl and extracted with EtOAc. The organic layer was dried over Na_2SO_4, filtered, and concentrated by rotary evaporation. The residue was purified by silica gel chromatography (0−10% MeOH in DCM with 0.1% AcOH) to provide the desired regioisomer as a white solid (1.93 g, 62%) followed by the undesired *N*1-isomer. Data for 2-(2*H*-1,2,3-triazol-2-yl)-5-methylbenzoic acid: ^{1}H NMR (500 MHz, DMSO-d_6) δ 12.98 (bs, 1H), 8.04 (s, 2H), 7.72−7.45 (m, 3H), 2.41 (s, 3H) ppm. HRMS-ESI m/z $[M + H]^+$ calcd for $C_{10}H_{10}N_3O_2$, 204.0768; found, 204.0769.

Benzyl (5*R*)-5-Methyl-4-[5-methyl-2-(2*H*-1,2,3-triazol-2-yl)-benzoyl]-1,4-diazepane-1-carboxylate (7). HCl gas was bubbled through a solution of 27 g (77 mmol) of (***R***)-**6** in 500 mL of EtOAc until the reaction reached approximately 50 °C, and the flask was capped and stirred for 15 min at room temperature. HCl gas was again bubbled through the solution, and the flask was capped and stirred 30 min at room temperature. The volatiles were removed by rotary evaporation to provide 22.3 g of a pale-yellow gum. This material was dissolved in 300 mL of DMF and treated with 2-(2*H*-1,2,3-triazol-2-yl)-5-methylbenzoic acid (15.9 g, 78 mmol), EDC (22.5 g, 118 mmol), 1-hydroxy-7-azabenzotriazole (12.8 g, 94 mmol), and *N*-methylmorpholine (43.1 mL, 392 mmol). After stirring at room temperature overnight, the reaction was partitioned between EtOAc and saturated aqueous $NaHCO_3$, the layers were separated, and the organic layer was washed with water, brine, dried over $MgSO_4$, filtered, and concentrated by rotary evaporation. The residue was purified by column chromatography with a gradient of 0−100% EtOAc in hexanes to provide 29.5 g [87% from (***R***)-**6**] of **7** as a colorless gum. LRMS = 434.5 (M + H). $[\alpha]_D$ = −34.4 (c = 1.0, chloroform). See the Supporting Information for a reproduction of the ^{1}H NMR spectrum at 25 °C in $CDCl_3$.

Acknowledgment. We thank Dr. Chuck Ross and Joan Murphy for HRMS analysis, Kim Michel for animal dosing, and Kristi Hoffman, Ken Anderson, and Mary Beth Young for pharmacokinetic analysis.

Supporting Information Available: Experimental procedures for compounds **8**−**13**, as well as reproductions of the ^{1}H and ^{13}C NMR spectra for key compounds. This material is available free of charge via the Internet at http://pubs.acs.org.

References

(1) Passarella, S.; Duong, M.-T. Diagnosis and treatment of insomnia. *Am. J. Health-Syst. Pharm.* **2008**, *65*, 927–934.

(2) Daley, M.; Morin, C. M.; LeBlanc, M.; Grégoire, J. P.; Savard, J.; Baillargeon, L. Insomnia and its relationship to health-care utilization, work absenteeism, productivity and accidents. *Sleep Med.* **2009**, *10*, 427–438.

(3) (a) Sullivan, S. S.; Guilleminault, C. Emerging drugs for insomnia: new frontiers for old and new targets. *Expert Opin. Emerging Drugs* **2009**, *14*, 411–422. (b) Renger, J. J. Overview of experimental and conventional pharmacological approaches in the treatment of sleep and wake disorders. *Curr. Top. Med. Chem.* **2008**, *8*, 937–953.

(4) Wafford, K. A.; Ebert, B. Emerging anti-insomnia drugs: tackling sleeplessness and the quality of wake time. *Nature Rev. Drug Discovery* **2008**, *7*, 530–540.

(5) FDA Requests Label Change for All Sleep Disorder Drug Products. *FDA News Release P07045*, March 14, 2007; http://www.fda.gov/NewsEvents/Newsroom/PressAnnouncements/2007/ucm108868.htm.

(6) Palomer, A.; Prinep, M.; Guglietta, A. Recent advances in the treatment of insomnia. *Annu. Rep. Med. Chem.* **2007**, *42*, 63–80.

(7) (a) Borja, N. L.; Daniel, K. L. Ramelteon for the treatment of insomnia. *Clin. Ther.* **2006**, *28*, 1540–1555. (b) Sateia, M. J.; Kirby-Long, P.; Taylor, J. L. Efficacy and clinical safety of ramelteon: an evidence-based review. *Sleep Med. Rev.* **2008**, *12*, 319–332.

(8) For a compilation of investigations carried out to identify the orexin system and define its physiological roles, see: *Hypocretins: Integrators of Physiological Functions*; de Lecea, L., Sutcliffe, J. G., Eds.; Springer: New York, 2005.

(9) (a) De Lecea, L.; Kilduff, T. S.; Peyron, C.; Gao, X.-B.; Foye, P. E.; Danielson, P. E.; Fukuhara, C.; Battenberg, E. L. F.; Gautvik, V. T.; Bartlett, F. S., II; Frankel, W. N.; Van Den Pol, A. N.; Bloom, F. E.; Gautvik, K. M.; Sutcliffe, J. G. The hypocretins: hypothalamus-specific peptides with neuroexcitatory activity. *Proc. Natl. Acad. Sci. U.S.A.* **1998**, *95*, 322–327. (b) Sakurai, T.; Amemiya, A.; Ishii, M.; Matsuzaki, I.; Chemelli, R.; Tanaka, H.; Williams, S. C.; Richardson, J. A.; Kozlowski, G. P.; Wilson, S.; Arch, J. R. S.; Buckingham, R. E.; Haynes, A. C.; Carr, S. A.; Annan, R. S.; McNulty, D. E.; Liu, W.; Terrett, J. A.; Elshourbagy, N. A.; Bergsma, D. J.; Yanagisawa, M. Orexins and orexin receptors: A family of hypothalamic neuropeptides and G-protein receptors that regulate feeding behavior. *Cell* **1998**, *92*, 573–585.

(10) (a) Chemelli, R. M.; Willie, J. T.; Sinton, C. M.; Elmquist, J. K.; Scammell, T.; Lee, C.; Richardson, J. A.; Williams, S. C.; Xiong, Y.; Kisanuki, Y.; Fitch, T. E.; Nakazato, M.; Hammer, R. E.; Saper, C. B.; Yanagisawa, M. Narcolepsy in orexin knockout mice: molecular genetics of sleep regulation. *Cell* **1999**, *98*, 437–451.

(11) Willie, J. T.; Chemelli, R. M.; Sinton, C. M.; Tokita, S.; Williams, S. C.; Kisanuki, Y. Y.; Marcus, J. N.; Lee, C.; Elmquist, J. K.; Kohlmeier, K. A.; Leonard, C. S.; Richardson, J. A.; Hammer, R. E.; Yanagisawa, M. Distinct narcolepsy syndromes in orexin receptor 2 and orexin null mice: molecular genetic dissection of non-REM and REM sleep regulatory processes. *Neuron* **2003**, *38*, 715–730.

(12) Lin, L.; Faraco, F.; Li, R.; Kadotani, H.; Rogers, W.; Lin, X.; Qiu, X.; de Jong, P. J.; Nishino, S.; Mignot, E. The sleep disorder canine narcolepsy is caused by a mutation in the hypocretin receptor 2 gene. *Cell* **1999**, *98*, 365–376.

(13) (a) Thannickal, T. C.; Moore, R. Y.; Nienhuis, R.; Ramanathan, L.; Gulyani, S.; Aldrich, M.; Cornford, M.; Siegel, J. M. Reduced number of hypocretin neurons in human narcolepsy. *Neuron* **2000**, *27*, 469–474. (b) Crocker, A.; Espana, R. A.; Papadopoulon, M.; Saper, C. B.; Faraco, J.; Sakurai, T.; Honda, M.; Mignot, E.; Scammell, T. E. Concomitant loss of dynorphin, Narp and orexin in narcolepsy. *Neurology* **2005**, *65*, 1184–1188. (c) Blouin, A. M.; Thannickal, T. E.; Worley, P. F.; Baraban, J. M.; Reti, I. M.; Siegel, J. M. Narp immunostaining of human hypocretin (orexin) neurons: loss in narcolepsy. *Neurology* **2005**, *65*, 1189–1192.

(14) Akanmu, M. A.; Honda, K. Selective stimulation of orexin receptor type 2 promotes wakefulness in freely behaving rats. *Brain Res.* **2005**, *1048*, 138–145.

(15) (a) Selbach, O.; Eriksson, K. S.; Haas, H. L. Drugs to interfere with orexins (hypocretins). *Drug News Perspect.* **2003**, *16*, 669–681. (b) Baumann, C. R.; Bassetti, C. L. Hypocretins (orexins): clinical impact of the discovery of a neurotransmitter. *Sleep Med. Rev.* **2005**, *9*, 253–268. (c) Boss, C.; Brisbare-Roch, C.; Jenck, F.; Aissaoui, H.; Koberstein, R.; Sifferlen, T.; Weller, T. Orexin receptor antagonism: A new principle in neuroscience. *Chemia* **2008**, *62*, 974–979. (d) Boss, C.; Brisbare-Roch, C.; Jenck, F. Biomedical application of orexin/hypocretin receptor ligands in neuroscience. *J. Med. Chem.* **2009**, *52*, 891–903.

(16) (a) McAtee, L. C.; Sutton, S. W.; Rudolph, D. A.; Li, X.; Aluisio, L. E.; Phoung, V. K.; Dvorak, C. A.; Lovenberg, T. W.; Carruthers, N. I.; Jones, T. K. Novel substituted 4-phenyl-[1,3]dioxanes: potent and selective orexin 2 (OX_2R) antagonists. *Bioorg. Med. Chem. Lett.* **2004**, *14*, 4225–4229. (b) Bingham, M. J.; Cai, J.; Deehan, M. R. Eating, sleeping and rewarding: orexin receptors and their antagonists. *Curr. Opin. Drug Discovery Dev.* **2006**, *9*, 551–559. (c) Cai, J.; Cooke, F. E.; Sherborne, B. S. Antagonists of the orexin receptors. *Expert Opin. Ther. Patents* **2006**, *16*, 631–646. (d) Roecker, A. J.; Coleman, P. J. Orexin receptor antagonists: Medicinal chemistry and therapeutic potential. *Curr. Top. Med. Chem.* **2008**, *8*, 977–987.

(e) Bergman, J. M.; Roecker, A. J.; Mercer, S. P.; Bednar, R. A.; Reiss, D. R.; Ransom, R. W.; Harrell, C. M.; Pettibone, D. J.; Lemaire, W.; Murphy, K. L.; Li, C.; Preuksaritanont, T.; Winrow, C. J.; Renger, J. J.; Koblan, K. S.; Hartman, G. D.; Coleman, P. J. Proline bis-amides as potent dual orexin receptor antagonists. *Bioorg. Med. Chem. Lett.* **2008**, *18*, 1425–1430. (f) Cole, A. G.; Stroke, I. L.; Qin, L.-Q.; Hussain, Z.; Simhadri, S.; Brescia, M.-R.; Waksmunski, F. S.; Strohl, B.; Tellew, J. E.; Williams, J. P.; Saunders, J.; Appell, K. C.; Henderson, I.; Webb, M. L. Synthesis of (3,4-dimethoxyphenoxy)alkylamino acetamides as orexin-2 receptor antagonists. *Bioorg. Med. Chem. Lett.* **2008**, *18*, 5420–5423. (g) Aissaoui, H.; Koberstain, R.; Zumbrunn, C.; Gatfield, J.; Brisbane-Roch, C.; Jenck, F.; Treiber, A.; Boss, C. N-Glycine-sulfonamides as potent dual orexin 1/orexin 2 receptor antagonists. *Bioorg. Med. Chem. Lett.* **2008**, *18*, 5729–5733. (h) Sifferlen, T.; Boss, C.; Cottreel, E.; Koberstain, R.; Gude, M.; Aissaoui, H.; Weller, T.; Gatfield, J.; Brisbane-Roch, C.; Jenck, F. Novel pyrazolo-tetrahydropyridines as potent orexin receptor antagonists. *Bioorg. Med. Chem. Lett.* **2010**, *20*, 1539–1542. (i) Coleman, P. J.; Renger, J. J. Orexin receptor antagonists: a review of promising compounds patented since 2006. *Expert Opin. Ther. Patents* **2010**, *20*, 307–324.

(17) Dugovic, C.; Shelton, J. E.; Aluisio, L. E.; Fraser, I. C.; Jiang, X.; Sutton, S. W.; Bonaventure, P.; Yun, S.; Li, X.; Lord, B.; Dvorak, C. A.; Carruthers, N. I.; Lovenberg, T. W. Blockade of orexin-1 receptors attenuates orexin-2 receptor antagonism-induced sleep promotion in rat. *J. Pharmacol. Exp. Ther.* **2009**, *330*, 141–152.

(18) Owen, R. T.; Casteñer, R.; Bolós, J.; Estivill, C. Almorexant. *Drugs Future* **2009**, *34*, 5–10.

(19) Brisbare-Roch, C.; Dingemanse, J.; Koberstein, R.; Hoever, P.; Aissaoui, H.; Flores, S.; Mueller, C.; Nayler, O.; van Gerven, J.; de Haas, S. L.; Hess, P.; Qiu, C.; Buchmann, S.; Scherz, M.; Weller, T.; Fischli, W.; Clozel, M.; Jenck, F. Promotion of sleep by targeting the orexin system in rats, dogs and humans. *Nature Med.* **2007**, *13*, 150–155.

(20) New Data On Orexin Receptor Antagonist Almorexant Shows Therapeutic Potential To Restore Normal Physiological Sleep In Insomnia Patients. *Medical News Today* Sep 04, 2007; http://www.medicalnewstoday.com/articles/81354.php.

(21) Following the observation of preclinical toxicity, GSK entered into a deal with Actelion to jointly develop and market Almorexant, see: http://www.bioworld.com/servlet/com.accumedia.web.Dispatcher?next=bioWorldHeadlines_article&forceid=48183

(22) Merck 2008 Annual Business Briefing—Final. *Goliath Business News* Dec 9, 2008; http://goliath.ecnext.com/coms2/gi_0199-9773483/Merck-2008-Annual-Business-Briefing.html.

(23) A Long Term Safety Study of MK4305 in Patients With Primary Insomnia.*ClinicalTrials.gov* 2009; http://clinicaltrials.gov/ct2/show/NCT01021813

(24) Whitman, D. B.; Cox, C. D.; Breslin, M. J.; Brashear, K. M.; Schreier, J. D.; Bogusky, M. J.; Bednar, R. A.; Lemaire, W.; Bruno, J. G.; Hartman, G. D.; Reiss, D. R.; Harrell, C. M.; Kraus, R. L.; Li, Y.; Garson, S. L.; Doran, S. M.; Prueksaritanont, T.; Li, C.; Winrow, C. J.; Koblan, K. S.; Renger, J. J.; Coleman, P. J. Discovery of a potent, CNS-penetrant orexin receptor antagonist based on an *N,N*-disubstituted-1,4-diazepane scaffold that promotes sleep in rats. *ChemMedChem* **2009**, *4*, 1069–1074.

(25) Further investigations by NMR spectroscopy, X-ray crystallography and molecular modeling revealed that **4** exists both in the solid state and solution in an unusual horseshoe- or U-shaped conformation characterized by a π-stacking interaction between the quinazoline and phenyl rings. (a) Cox, C. D.; McGaughey, G. B.; Bogusky, M. J.; Whitman, D. B.; Ball, R. G.; Winrow, C. J.; Renger, J. J.; Coleman, P. J. Conformational analysis of *N,N*-disubstituted-1,4-diazepane orexin receptor antagonists and implications for receptor binding. *Bioorg. Med. Chem. Lett.* **2009**, *19*, 2997–3001. We recently reported that bridged diazepane analogues, whose design and synthesis was inspired by the low energy conformation of **4**, are also potent DORAs that promote sleep in rats, see: (b) Coleman, P. J.; Schreier, J. D.; McGaughey, G. B.; Bogusky, M. J.; Cox, C. D.; Hartman, G. D.; Ball, R. G.; Harrell, C. M.; Reiss, D. R.; Prueksaritanont, T.; Winrow, C. J.; Renger, J. J. Design and synthesis of conformationally constrained N,N-disubstituted-1,4-diazepanes as potent orexin receptor antagonists. *Bioorg. Med. Chem. Lett.* **2010**, *20*, 2311–2315. (c) Coleman, P. J.; Schreier, J. D.; Roecker, A. J.; Mercer, S. P.; McGaughey, G. B.; Cox, C. D ; Hartman, G. D.; Harrell, C. M.; Reiss, D. R.; Garson, S. L.; Anderson, W. B.; Prueksaritanont, T.; Winrow, C. J.; Renger, J. J. Discovery of 3,9-diazabicyclo-[4.2.1]nonanes as potent orexin receptor antagonists with sleep-promoting activity in the rat. *Bioorg. Med. Chem. Lett.* **2010**, DOI: 10.1016/j.bmcl.2010.05.047

(26) Other vehicles studied included 0.5% aqueous methylcellulose, 10% Tween 80 in water, and 0.1 M citric acid.

(27) The position of oxidation is not known. For simplicity in visualization, oxidation at the 7-position of the core is shown.

(28) A large number of the cores made during this effort are described in Coleman, P. J.; Cox, C. D.; Roecker, A. J. Discovery of Dual Orexin Receptor Antagonists (DORAs) for the Treatment of Insomnia. *Curr. Top. Med. Chem.* in press.

(29) Dog pharmacokinetic "cassettes" where utilized wherein 5−6 test compounds plus a standard were dosed IV in DMSO, with the goal being to identify compounds with reduced IV clearance. Promising analogues were then repeated as both IV and PO singles. In general, the data obtained in cassette format was reproduced well in the IV singles. Though some exceptions were noted, this strategy led to a number of diazepanes with improved bioavailability.

(30) (a) Poppelsdorf, F.; Myerly, R. C. A novel synthesis of homopiperazine and its monomethyl derivatives. *J. Org. Chem.* **1961**, *26*, 131–134. (b) Benalil, A.; Guerin, A.; Carboni, B.; Vaultier, M. Synthesis of 2,3,6,7-tetrahydro- and 2,3,4,5,6,7-hexahydro-1H-1,4-diazepines via a tandem Michael-type addition-intramolecular aza-Wittig sequence. *J. Chem. Soc., Perkin Trans 1* **1993**, 1061–1064. (c) Subsequent to our work reported herein, an efficient synthesis of the mono-protected 5-methyldiazepane core was reported, see: Wlodarczyk, N.; Gilleron, P.; Millet, R.; Houssin, R.; Hénichart, J.-P. Synthesis of 1,4-diazepin-5-ones under microwave irradiation and their reduction products. *Tetrahedron Lett.* **2007**, *48*, 2583–2586.

(31) Leonard, J.; Lygo, B.; Procter, G. *Advanced Practical Organic Chemistry*; Blackie: New York, 1995; p 6.

(32) For instance, the (*S*)-antipode of compound **9** has OX_1R K_i = 54 nM and OX_2R K_i = 8.5 nM, corresponding to 8- and 18-fold losses in potency, respectively, relative to the (*R*)-antipode. We have confirmed the stereochemistry in the active series is (*R*) by both X-ray crystallography using anomalous dispersion, as well as an asymmetric synthesis starting from the chiral pool.

(33) In general, installation of the tolyl methyl group on the benzamide increases potency on both receptors, but has a greater effect on OX_1R potency.

(34) We have found that a vehicle of 20% TPGS in water to be an excellent vehicle for improving exposure of BCS class II molecules such as the diazepanes described herein and is also highly compatible with our sleep studies. For a study of the effects that TPGS has on oral absorption, see: Varma, M. V. S.; Panchagnula, R. Enhanced oral paclitaxel absorption with vitamin E-TPGS: effect on solubility and permeability in vitro, in situ and in vivo. *Eur. J. Pharm. Sci.* **2005**, *25*, 445–453.

(35) Brain, plasma, and CSF concentrations were measured following a 30 min continuous IV infusion of **10** at 0.25, 0.75, and 1.5 mg/kg in 25% hydroxypropyl-β-cyclodextrin.

(36) (a) Evans, D. C.; Watt, A. P.; Nicoll-Griffith, D. A.; Baillie, T. A. Drug−protein adducts: an industry perspective on minimizing the potential for drug bioactivation in drug discovery and development. *Chem. Res. Toxicol.* **2004**, *17*, 3–16.(b) Kumar, S.; Baillie, T. A. Minimizing metabolic activation in drug discovery in *Handbook of Drug Metabolism*, 2nd ed.; Pearson, P. G., Wienkers, L. C., Eds.; Informa Healthcare: New York, 2009; Chapter 23.

(37) See the Experimental Section for details.

(38) GSH-adducts were identified that had a mass spectral signal corresponding to loss of the fluorine atom, suggesting the fluoroquinazoline as a site of bioactivation. The GSH-adduct/IS ratio of compound **4** is 5.0, suggesting that the nonfluorinated quinazoline also likely undergoes bioactivation and subsequent trapping with GSH.

(39) As with diazepane DORA **4**, solution NMR studies of **3** indicate a very complex situation with several low energy conformations in equilibrium. Studies are underway to characterize the low energy conformations of **3** and how they fit with our proposed bioactive conformation model.[25]

(40) Brain, plasma, and CSF concentrations were measured following a 30 min continuous IV infusion of **3** at 0.25, 0.75, and 1.5, and 2.0 mg/kg in 25% hydroxypropyl-β-cyclodextrin. Brain/plasma ratios ranged from 0.6−1.2 and the CSF/plasma ratios ranged from 0.007−0.017. When dosed at 10 mg/kg PO in 20% TPGS, at 1 h post dose the brain/plasma ratio was 0.7 and the CSF/plasma ratio was 0.007.

(41) A manuscript in preparation will describe the pharmacology of **3** in more detail, including analysis of its dose-dependent effects on sleep in rats, dogs, and monkeys. Winrow, C. J. unpublished results.

(42) The identities of **14**−**16** were confirmed by independent synthesis.

(43) Kunapuli, P.; Ransom, R.; Murphy, K. L.; Pettibone, D. J.; Kerby, J.; Grimwood, S.; Zuck, P.; Hodder, P.; Lacson, R.; Hoffman, I.; Inglese, J.; Strulovici, B. Development of an intact cell reporter gene β-lactamase assay for G-protein coupled receptors for high-throughput screening. *Anal. Biochem.* **2003**, *314*, 16–29.

(44) Mosser, S. D.; Stanley, L.; Gaul, S. L.; Bednar, B.; Koblan, K. S.; Bednar, R. A. Automation of in vitro dose-inhibition assays using the Tecan Genesis and an integrated software package to support the drug discovery process. *J. Assoc. Lab. Autom.* **2003**, *8*, 54–62.

(45) (a) Alvarino, F.; Monti, J. M.; Jantos, H.; Monti, D. Effect of SX-3228, a selective ligand for the BZ1 receptor, on sleep and waking during the light−dark cycle in the rat. *Braz. J. Med. Biol. Res.* **1999**, *32*, 1007–1014. (b) Monti, J. M.; Jantos, H.; Monti, D. Increase in waking and reduction of NREM and REM sleep after nitric oxide synthase inhibition: prevention with GABAA or adenosine A1 receptor agonists. *Behav. Brain Res.* **2001**, *123*, 23–35.

(46) Lazer, E. S.; Miao, C. K.; Wong, H.-C.; Sorcek, R.; Spero, D. M.; Gilman, A.; Pal, K.; Behnke, M.; Graham, A. G.; Watrous, J. M.; Homon, C. A.; Nagel, J.; Shah, A.; Guindon, Y.; Farina, P. R.; Adams, J. Benzoxazolamines and benzothiazolamines: Potent, enantioselective inhibitors of leukotriene biosynthesis with a novel mechanism of action. *J. Med. Chem.* **1994**, *37*, 913–923.